

**Transient response of blue organic
electroluminescence devices with short
fluorescence lifetime of substituted phenyl/vinyl
compound as an emissive layer**

Takeshi Fukuda and Masakazu Ohashi

Optics and Electronics Laboratory, Fujikura Ltd.

Mutsuzaki 1440, Sakura, Chiba 285-8550, Japan

Bin Wei, Tomoko Okada, Musubu Ichikawa and Yoshio Taniguchi

Department of Functional Polymer Science, Shinshu University,

Tokida 3-15-1, Ueda, Nagano 386-8567, Japan

We have demonstrated a short fluorescence lifetime of substituted phenyl/vinyl compound, 1,4-bis[2-[4-[N,N-di(p-tolyl)amino]phenyl]vinyl]benzene (DSB). The fluorescence lifetime of the 0.5-mol% DSB doped 4,4'-bis(9-carbazolyl)biphenyl film is 1.2 ns, which is desirable for organic light-emitting diode (OLED) light sources for optical interconnect applications. We have also examined frequency dependences on the electroluminescence (EL) intensity of the OLED and the photoluminescence (PL) intensity of the DSB film. The -3 dB cutoff frequency of the EL intensity is about 3 MHz for the optimized device, and the -3 dB cutoff frequency of the PL intensity is about 160 MHz for the optically pumping DSB film. © 2007 Optical Society of America

OCIS codes: 160.4890, 250.5230, 130.3120, 230.6080, 230.3670

Organic light-emitting diodes (OLEDs) and organic photo-diodes (OPDs) have been expected to be applied in optical interconnects because of their low-cost fabrication process and flexibility^{1,2} In addition, high-luminance blue OLEDs are required to realize the efficient signal transmission in the optical interconnect. Furthermore, blue OLEDs also can be used as an excitation source to organic films for realizing organic solid-state laser,³ and as fluorescence sensors to monitor environmental or biochemical processes in vitro and in vivo.⁴

However, blue OLEDs were widely reported to have relatively low luminance efficiencies due to the large energy band-gap of blue emission materials, which inhibits the carrier injection after applying the bias voltage^{5,6,7,8} Some approaches to facilitating the carrier injection to the blue emission material have been investigated, such as the use of the low work-function cathode^{9,10} of the high-mobility electron transport material,¹¹ and of the host-guest system as a light-emitting layer (EML)^{12,13,14} Moreover, a short fluorescence lifetime (FL) of the EML is necessary to achieve the fast transient response of the OLED.

In this paper, we have investigated the FL of the DSB doped 4,4'-bis(9-carbazolyl)biphenyl (CBP) film as a function of the doping concentration. Furthermore, by utilizing DSB in CBP as the EML of the OLED, current density-voltage-luminance characteristics and transient responses of devices were evaluated under DC and high-frequency sine wave voltages, respectively. We have also studied the frequency dependence on the photoluminescence (PL) intensity of the DSB film.

We measured FLs of 100 nm DSB doped CBP films with different concentrations. The FL was measured under second harmonics (peak wavelength = 380 nm) from a

high-repetition-rate Ti: Sapphire femtosecond laser, and the radiated PL was captured with a streak camera. Mono-exponential fitting was employed to derive the FL.

Using DSB doped CBP as the EML, we fabricated two devices. Figure 1 shows device structures and energy diagrams of devices A and B. We used 4,4'-bis[N-(1-naphthyl)-N-phenyl-amino]biphenyl as a hole transport layer, DSB in CBP as an EML and tris(8-hydroxyquinoline)aluminum (Alq_3) as an electron transport layer (ETL), subsequently, upon the ITO-coated glass substrate. For comparison, we used bathocuproine (BCP) as a hole-blocking layer (HBL) between the EML and the ETL in the device B. An electron injection layer of LiF with 0.4 nm thickness and a cathode of Al were evaporated on the top of organic layers.

In addition, highest occupied molecular orbital (HOMO) levels of each layers were measured with the photoelectron emission spectrometer (AC-3, Riken Keiki). The lowest unoccupied molecular orbital (LUMO) level was estimated from the HOMO level and the band-gap which was determined by the visible absorption spectrum of the neat thin film.

We have also investigated transient responses of OLEDs with a small-area under a high-frequency sine wave voltage, which was generated by the programmable FM/AM standard signal generator (SG-7200, KENWOOD). The EL intensity was measured by the avalanche photo-diode. Furthermore, we also tested the frequency dependence on the PL intensity of the DSB film pumped by the blue laser diode (NDHV220APAE1, NICHIA Corp.).

Figure 2 shows FLs of blend films with different DSB concentration. We found that the FL of DSB in CBP is short compared to that of the widely used green emitter

Alq₃ of which the FL is about 16 ns. The FL varies with the doping concentration, and it decreases with extra amount of fluorescent dye in the host due to the effect of concentration quenching.¹⁵ The shortest FL of the blend film can reach 1.2 ns at the DSB concentration of 0.5-mol% . However, the FL starts to decrease after a certain DSB concentration of 4.0-mol% . We assume that the exciton interaction between the nearest neighbor acceptor molecules may be responsible for the fluorescence quenching.

Figure 2 also shows the relationship between the current efficiency at the current density of 100 mA/cm² and the DSB concentration in CBP. We found that the change in the concentration of DSB in CBP affects the device performance, and the optimized concentration is found to be 0.5-mol% for achieving the enhanced device performance. The current efficiency is found to decrease with the increase of dopant amount in the EML, which is contributed by the dopant molecule's aggregation quenching.

Figure 3 (a) reveals that the use of the HBL can improve the current density and the luminance significantly. The maximum luminance of the device B reaches 16500 cd/m² at 12.5 V, while that of the device A is only 12000 cd/m² at 14.5 V. Moreover, external quantum efficiencies of devices A and B reach 1.1 % and 2.2 % at the current density of 1.6 mA/cm², respectively. This indicates that the use of BCP as the HBL can prevent leakage of holes into the ETL, and meanwhile facilitate the electron injection from the ETL into the EML. The barrier height to block the holes leakage is estimated by the difference of HOMO levels between the EML and the adjacent organic layer, such as the ETL for the device A or the HBL for the device B. There is no block barrier between the EML and the ETL for the device A, while

the barrier height is 0.4 eV for the device B.

In addition, the electron injection efficiency is closely related to the difference of LUMO levels between adjacent two organic layers. The barrier height between the EML and the HBL is 0.3 eV to inject electrons into the EML for the device B, while the barrier height between the EML and the ETL is 0.7 eV for the device A. Accordingly, the efficient electron injection is assumed to result in a balanced hole-electron pair recombination. As a result, the external quantum efficiency of the device B is higher than that of the device A.

EL Spectra of devices A and B are also found to be different as shown in Fig. 3 (b). The peak EL emission of the device B is 472 nm, while there is a shoulder at the wavelength of 508 nm. It is only the emitting of DSB molecules due to the hole block effect of BCP between the ETL (Alq_3) and the EML (DSB). On the other hand, the center wavelength of the EL spectrum of the device A is about 480 nm. Meanwhile, the second peak emission at 512 nm of the device A is higher than that of the device B. We assume that the second peak is attributed to the EL emission from Alq_3 molecule, which is used as the ETL. The PL spectrum of the Alq_3 film is also shown in Fig. 3 (b), whose peak wavelength is located near the second peak of the EL spectrum of the device A.

Figure 4 shows the logarithmic plot of the EL intensity against the frequency of the applied sine wave voltage at the amplitude of 8 V and bias voltage of 8 V for devices A and B. The EL intensity at the frequency of 3 MHz relative to that of 100 kHz are 0.46 and 0.41 for devices B with 0.4-mm^2 and 0.6-mm^2 active areas, respectively. The decrease in the active area causes the increase in the response time

of devices, because the capacitance of devices can be reduced with a smaller size OLEDs.¹⁶ And, we have also revealed the BCP effect of the frequency dependence on the EL intensity, and it increases by inserting of the BCP layer. The EL intensity at the frequency of 3 MHz relative to that of 100 kHz are 0.46 and 0.52 for devices A and B with 0.4-mm² active areas, respectively. The -3 dB cutoff frequency of the device B is about 3 MHz. This result indicates that the BCP layer blocks hole transportation into the Alq₃ layer, and the FL of Alq₃ is about 16 ns, which is longer than that of the DSB doped in CBP layer. As a result, transient properties of OLEDs increase by inserting the BCP layer as shown in Fig. 4.

Figure 4 also shows the frequency dependence on the PL intensity of the DSB film. Without the limitation of the capacitance as well as the transient delay of the injection and the transportation by carriers,¹⁷ the maximum -3 dB cutoff frequency can reach about 160 MHz, which is the fastest reported for fluorescent organic films.

In conclusion, we have investigated PL and EL characteristics of short FL films. The FL is only 1.2 ns for this blend film when the content of DSB in CBP is 0.5-mol% . Utilizing the DSB doped CBP film as the EML and BCP as the HBL, we have developed the highly efficient blue OLED, and the maximum luminance of 16500 cd/m² and the maximum external quantum efficiency of 2.2 % have been obtained. Furthermore, we have realized that the -3 dB cutoff frequency of the optimized device and the PL of the DSB film are 3 MHz and 160 MHz, respectively. The potential application of the bright blue device for optical interconnects is also demonstrated.

List of Figure Captions

Fig. 1. Scheme of energy diagrams and device structures of devices (a) A and (b) B.

Fig. 2. The influence of the concentration of DSB in CBP on the FL and the current efficiency at the current density of 100 mA/cm².

Fig. 3 . (a) Current density-voltage-luminance characteristics of devices A and B, and (b) their EL spectra and the PL spectrum of the Alq₃ film.

Fig. 4. The logarithmic plot of the EL intensity of the OLED versus the frequency of the applied sine wave voltage at the amplitude of 8 V with the bias voltage of 8 V, and the frequency dependence on the PL intensity pumped by the blue laser diode.

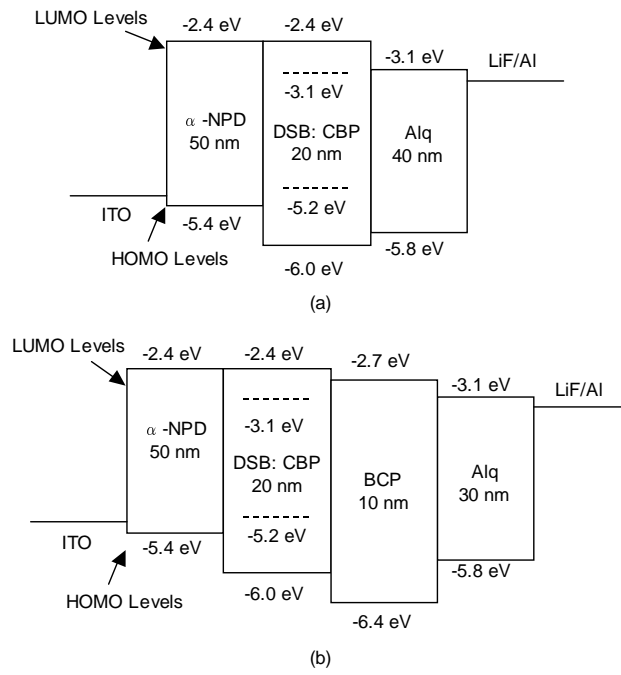


Fig. 1. Scheme of energy diagrams and device structures of devices (a) A and (b) B.

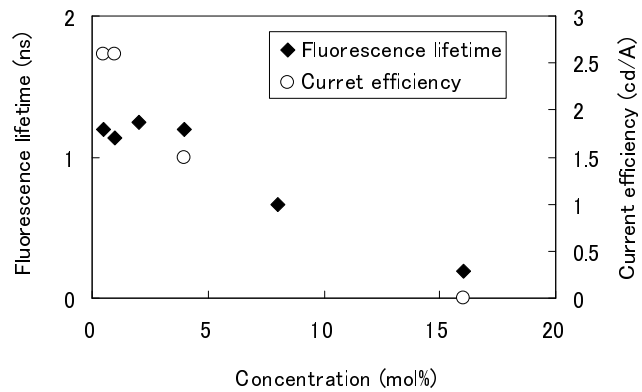


Fig. 2. The influence of the concentration of DSB in CBP on the FL and the current efficiency at the current density of 100 mA/cm².

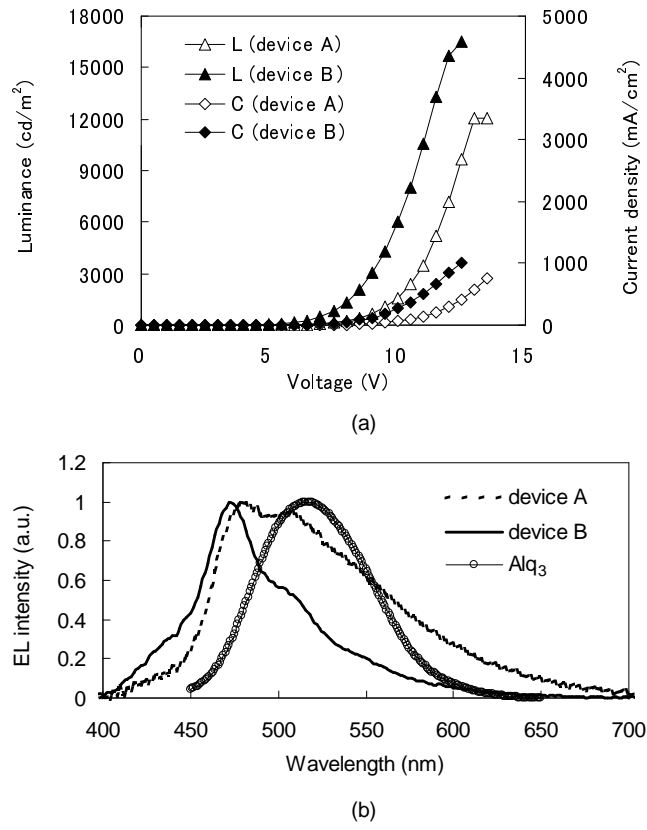


Fig. 3. (a) Current density-voltage-luminance characteristics of devices A and B, and (b) their EL spectra and the PL spectrum of the Alq₃ film.

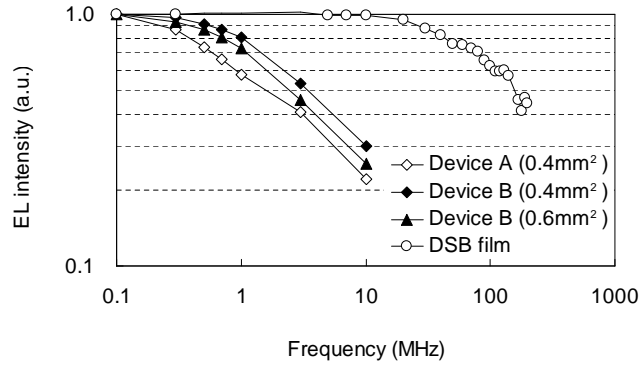


Fig. 4. The logarithmic plot of the EL intensity of OLED devices versus the frequency of the applied sine wave voltage at the amplitude of 8 V with the bias voltage of 8 V, and the frequency dependence on the PL intensity pumped by the blue laser diode.

References

1. H. Kajii, T. Tsukagawa, T. Taneda, K. Yoshino, O. Ozaki, A. Fujii, M. Hikita, S. Tomaru, S. Imamura, H. Takenaka, J. Kobayashi, F. Yamamoto, and Y. Omori, *Jpn. J. Appl. Phys.* **41**, 2746-2748 (2002).
2. T. Morimune, H. Kajii, and Y. Omori, *Jpn. J. Appl. Phys.* **45**, 546-549 (2006).
3. B. Wei, T. Fukuda, N. Kobayashi, M. Ichikawa, T. Koyama, and Y. Taniguchi, *Opt. Exp.* **14**, 9436-9443 (2006).
4. R. Shinar, Z. Zhou, B. Choudhury, L. B. Tabatabai, and J. Shinar, *International Society for Optical Engineering* **5588**, 59-69 (2005).
5. C. Hosokawa, N. Kawasaki, S. Sakamoto, and T. Kusumoto, *Appl. Phys. Lett.* **61**, 2503-2505 (1992).
6. I. D. Parker, Q. Pei, and M. Marrocco, *Appl. Phys. Lett.* **65**, 1272-1274 (1994).
7. Y. Yang, Q. Pei, and A. J. Heeger, *J. Appl. Phys.* **79**, 934-939 (1996).
8. A. W. Grice, D. D. C. Bradley, M. T. Bernius, M. Inbasekaran, W. W. Wu, and E. P. Woo, *Appl. Phys. Lett.* **73**, 629-631 (1998).
9. S. E. Shaheen, G. E. Jabbour, M. M. Morrell, Y. Kawabe, B. Kippelen, N. Peyghambarian, M.-F. Nabor, R. Schlaf, E. A. Mash, and N. R. Armstrong, *J. Appl. Phys.* **84**, 2324-2327 (1998).
10. B. J. Chen, X. W. Sun, K. S. Wong, and X. Hu, *Opt. Exp.* **13**, 26-31 (2005).
11. L. C. Palilis, A. Makinen, M. Uchida, and Z. H. Kafafi, *Appl. Phys. Lett.* **82**, 2209-2211 (2003).
12. C. Hosokawa, H. Higashi, H. Nakamura, and T. Kusumoto, *Appl. Phys. Lett.* **67**,

- 3853-3855 (1995).
13. Y. Z. Wu, X. Y. Zheng, W. Q. Zhu, R. G. Sun, X. Y. Jiang, Z. L. Zhang, and S. H. Xu, *Appl. Phys. Lett.* **83**, 5077-5079 (2003).
 14. R. J. Tseng, R. C. Chiechi, F. Wudl, Y. Yang, *Appl. Phys. Lett.* **88**, 093512 (2006).
 15. Z. H. Kafafi, H. Murata, L. C. Picciolo, H. Mattoussi, C. D. Merritt, Y. Lizimu, and J. Kido, *Pure Appl. Chem.*, **71**, 2085-2094 (1999).
 16. K. Kajii, T. Tsukagawa, T. Taneda, Y. Omori, *IEICE TRANS. ELECTRON.* **E85-C**, 1245-1246 (2002).
 17. B. Wei, K. Furukawa, J. Amagai, M. Ichikawa, T. Koyama, and Y. Taniguchi, *Semicond. Sci. Technol.* **19**, L56-L59 (2004).